

- 1 Atmospheric chemistry of volatile methyl siloxanes:
- 2 Kinetics and products of oxidation by OH radicals
- 3 and Cl atoms

4 *Mitchell W. Alton<sup>1</sup> and Eleanor C. Browne\*<sup>1</sup>*

## 7 ABSTRACT

8 Volatile methyl siloxanes (VMS) are ubiquitous anthropogenic pollutants that have recently come  
 9 under scrutiny for their potential toxicity and environmental persistence. In this work, we  
 10 determined the rate constants for oxidation by OH radicals and Cl atoms at  $297 \pm 3$  K and  
 11 atmospheric pressure in Boulder, CO (~860 mbar) of hexamethyldisiloxane (L2),  
 12 octamethyltrisiloxane (L3), decamethyltetrasiloxane (L4), dodecamethylpentasiloxane (L5),  
 13 hexamethylcyclotrisiloxane (D3), octamethylcyclotetrasiloxane (D4), and  
 14 decamethylcyclopentasiloxane (D5). Measured rate constants with OH radicals were  $(1.20 \pm 0.09)$   
 15  $\times 10^{-12}$ ,  $(1.7 \pm 0.1) \times 10^{-12}$ ,  $(2.5 \pm 0.2) \times 10^{-12}$ ,  $(3.4 \pm 0.5) \times 10^{-12}$ ,  $(0.86 \pm 0.09) \times 10^{-12}$ ,  $(1.3 \pm 0.1)$   
 16  $\times 10^{-12}$ , and  $(2.1 \pm 0.1) \times 10^{-12}$   $\text{cm}^3 \text{ molec}^{-1} \text{ s}^{-1}$ , for L2, L3, L4, L5, D3, D4, and D5 respectively.  
 17 The rate constants for reactions with Cl atoms with the same compounds were  $(1.44 \pm 0.05) \times 10^{-12}$

18  $^{10}$ ,  $(1.85 \pm 0.05) \times 10^{-10}$ ,  $(2.2 \pm 0.1) \times 10^{-10}$ ,  $(2.9 \pm 0.1) \times 10^{-10}$ ,  $(0.56 \pm 0.05) \times 10^{-10}$ ,  $(1.16 \pm 0.08)$   
19  $\times 10^{-10}$ , and  $(1.8 \pm 0.1) \times 10^{-10}$   $\text{cm}^3 \text{ molec}^{-1} \text{ s}^{-1}$ , respectively. Substituent factors of  $F(-\text{Si}(\text{CH}_3)_2\text{OR})$   
20 and  $F(-\text{SiCH}_3(\text{OR})_2)$  are proposed for use in AOPWIN, a common model for OH radical rate  
21 constant estimations. Cl atoms can remove percentage levels of VMS globally with potentially  
22 increased importance in urban areas.

23 **1 INTRODUCTION**

24 Each year, an estimated two million of tons of linear and cyclic volatile methyl siloxanes (VMS)  
25 are produced globally for use in consumer and industrial applications including as components of  
26 personal care products, household cleaners, lubricants, and as starting materials for silicone  
27 polymers.<sup>1–4</sup> These high production values coupled with the prevalence of VMS in consumer  
28 products has led to substantial industrial, governmental, and academic interest in the  
29 environmental behavior and fate of VMS.<sup>1–18</sup> Despite this interest, there remains gaps in our  
30 understanding of the environmental fate of VMS. For instance, a recent study found discrepancies  
31 between modeled and measured VMS concentrations, particularly in remote environments, and  
32 proposed that the model is missing gas phase removal pathways for VMS.<sup>13</sup>

33 Environmental release of VMS is thought to be centered in urban areas owing to the prevalence  
34 of VMS in personal care and other consumer products.<sup>19–21</sup> Due to the extremely low water  
35 solubility and high vapor pressure of VMS, more than 90% of the D5 in cosmetic products is  
36 released to the atmosphere.<sup>15</sup> Consequently, gas phase chemistry plays a critical role in the  
37 environmental processing of VMS. The gas phase chemistry of VMS compounds is thought to be  
38 driven by hydroxyl radicals (OH), which oxidize VMS on the time scale of several days.<sup>5–9,16–18</sup>  
39 The resulting VMS oxidation products, such as silanols (where a methyl group has been substituted

40 with a hydroxyl group), have lower vapor pressures and higher water solubility than the parent  
41 VMS, though the environmental effects have not been as well studied.<sup>1,12</sup> Additionally, recent  
42 ambient measurements<sup>10</sup> and laboratory studies<sup>11,22,23</sup> indicate that oxidized VMS compounds may  
43 be present in new particles and contribute to secondary organic aerosol formation, thus negatively  
44 affecting air quality. Therefore, an understanding of the rates and products of VMS gas phase  
45 transformations is crucial to comprehending the environmental fate of these compounds.

46 Despite multiple measurements of the oxidation rate of various VMS by OH,<sup>5–9,16,18</sup> uncertainty  
47 remains regarding these rates constants. Rate constants of the smaller VMS have been measured  
48 more times and with smaller uncertainties than the larger VMS such as D5, which are more  
49 prevalent in personal care products and more likely to be emitted into the atmosphere.  
50 Furthermore, Cl atom-initiated VMS oxidation has been largely ignored with the only prior rate  
51 determination being for L2.<sup>17</sup> Even low concentrations of Cl atoms shorten the lifetime of volatile  
52 gases due to much faster rates of reaction as compared to OH radicals. Oxidation by Cl atoms has  
53 traditionally been thought to be important only in the polar and marine boundary layer; however,  
54 recent observations of elevated Cl atom concentrations in urban continental airmasses suggest that  
55 Cl atom chemistry may influence urban photochemistry<sup>24–26</sup> and thus may be important for VMS  
56 processing.

57 In order to improve the understanding of VMS atmospheric lifetimes and degradation, we  
58 measured the rate constants of hexamethyldisiloxane (L2), octamethyltrisiloxane (L3),  
59 decamethyltetrasiloxane (L4), dodecamethylpentasiloxane (L5), hexamethylcyclotrisiloxane  
60 (D3), octamethylcyclotetrasiloxane (D4), and decamethylcyclopentasiloxane (D5) with OH  
61 radicals and Cl atoms at room temperature and local atmospheric pressure (~860 mbar) using the  
62 method of relative rates. Structures of the VMS used in these experiments are shown in Figure S1.

63 Although cyclic VMS have been detected in the ambient atmosphere in concentrations between  
64 one and three orders of magnitude higher than linear VMS,<sup>2,27,28</sup> linear VMS have been detected  
65 in indoor dust at approximately equal concentrations as cyclic VMS.<sup>29</sup> As D4 is one of the most  
66 abundant VMS in the atmosphere and is potentially more toxic than D5,<sup>2,12</sup> the products formed  
67 from D4 oxidation were also analyzed. Some oxidation products that were detected had the same  
68 molecular formulas as compounds reported in other studies, such as the silanol and formate ester  
69 products, but with temporal evolutions that indicate a different formation mechanism than  
70 previously suggested.<sup>8,17</sup> With these measurements, we derive updated structure-activity  
71 relationship factors for VMS oxidation by the OH radical and estimate the relative importance of  
72 Cl atom and OH radical oxidation to VMS lifetime.

73

## 74 **2 MATERIALS AND METHODS**

75 Experiments were performed in a ~1m<sup>3</sup> Teflon<sup>®</sup> 200A FEP film chamber at room temperature  
76 (297 ± 3 K) and local ambient pressure (~860 mbar). The chamber was flushed with zero air  
77 (AADCO Instruments, 737 series) for at least fifteen hours between sets of experiments. This was  
78 sufficient to ensure VMS concentrations were below the limit of detection (e.g. 5 pptv for D4, 1 s  
79 measurements). VMS and reference compounds were introduced to the chamber by flowing zero  
80 air for ~5-15 seconds over the headspace of pure compounds to achieve mixing ratios between ~2-  
81 5 ppbv. For OH radical experiments, ozone was formed by passing zero air over a mercury arc  
82 lamp (Jelight, 78-2046-7) and into the chamber until it reached a mixing ratio of ~300 ppbv as  
83 measured by a O<sub>3</sub> monitor (2B Technologies, 202). For Cl atom experiments, ~40 ppbv of Cl<sub>2</sub> was  
84 introduced into the chamber using a permeation device (Vici Metronics). The chamber was kept  
85 at less than 2% RH in the Cl atom experiments and between 20%-25% relative humidity for OH

86 radical experiments by passing zero air through a bubbler with Milli-Q water (Millipore-Sigma).  
87 As there is no fan installed in the chamber, all reactants were allowed to mix in the chamber for  
88 10 minutes before oxidation was initiated. Control experiments confirmed that VMS and reference  
89 compounds exhibited negligible decay when exposed to either the lights or the oxidant precursors  
90 independently. Wall loss was also determined to be negligible for the parent VMS compounds. A  
91 scanning electrical mobility spectrometer (SEMS; Brechtel Manufacturing Inc., Hayward, CA  
92 model SEMS 2100) was used on selected experiments; nucleation events were not observed during  
93 these experiments.

94 For OH radical experiments, four 254 nm lights (General Electric, G36T8) positioned below the  
95 chamber were used to photolyze ozone into O(<sup>1</sup>D); subsequent reaction with H<sub>2</sub>O formed OH  
96 radicals. For Cl atom experiments, ten 370 nm lights (General Electric, F40BL) were used to  
97 photolyze Cl<sub>2</sub> generating Cl atoms. The average concentrations of OH radicals and Cl atoms  
98 generated are estimated to be  $5 \times 10^8$  molecules cm<sup>-3</sup> and  $1 \times 10^6$  molec cm<sup>-3</sup>, respectively, from the  
99 measured decrease in the reference compounds' signals.

100 VMS and reference compounds were measured using a High-Resolution Chemical Ionization  
101 Time-of-Flight Mass Spectrometer (CIMS; Aerodyne Research, Inc. and Tofwerk AG) interfaced  
102 to the chamber. Gases were sampled directly from the chamber at 400 sccm and mixed with a 1.3  
103 slpm dilution flow before being sampled by the CIMS. Details regarding CIMS operation are  
104 provided in section 2 of the supporting information. Briefly, the CIMS utilized protonated toluene  
105 (99.5%, Fisher Scientific) as the reagent ion. Although toluene is frequently used as a dopant in  
106 atmospheric pressure chemical ionization studies (APCI),<sup>30</sup> to our knowledge, this is the first use  
107 of toluene reagent ions under conditions where reagent ion and analyte ion generation are

108 physically separated, allowing a quantitative measurement. All compounds of interest were  
109 detected as  $\text{MH}^+$  ions.

110 Rate constants for the oxidation of L2 (98%, Alfa Aesar), L3 (97%, TCI), L4 (97%, Sigma-  
111 Aldrich), L5 (97%, Sigma-Aldrich), D3 (98%, Acros Organics), D4 (98%, Acros Organics), D5  
112 (97%, Sigma-Aldrich) by OH radicals and Cl atoms were measured in triplicate using the relative  
113 rate method.<sup>31</sup> The advantage of the relative rate method is that it depends only on the relative  
114 concentration changes; an absolute calibration is unnecessary. In this method, the loss rate of a  
115 reference compound with a well-established OH radical (or Cl atom) rate constant is monitored  
116 and compared to the loss rate of VMS. Assuming the loss of both the VMS and the reference  
117 compound is due solely to reaction with OH radicals (or Cl atoms), the rate constants for VMS  
118 oxidation and reference compound oxidation are related by the following equation:

$$119 \ln\left(\frac{[\text{Siloxane}]_0}{[\text{Siloxane}]_t}\right) = \frac{k_{\text{Siloxane}}}{k_{\text{Reference}}} * \ln\left(\frac{[\text{Reference}]_0}{[\text{Reference}]_t}\right) \quad (1)$$

120 where  $[\text{VMS}]_0$ ,  $[\text{Reference}]_0$ ,  $[\text{VMS}]_t$ , and  $[\text{Reference}]_t$  are the VMS and reference compound  
121 signals before oxidation and at time  $t$ , and  $k_{\text{VMS}}$  and  $k_{\text{Reference}}$  are the OH radical (or Cl atom) rate  
122 constants for the VMS and reference compound, respectively. Propionic acid (99.5%, Fisher  
123 Scientific) and methyl ethyl ketone (MEK, 99%, Fisher Scientific) served as reference compounds  
124 for OH radical oxidation experiments, while MEK and diethyl ether (ether, 99%, VWR) were used  
125 for Cl atom experiments. All chemicals were used as received without further purification.

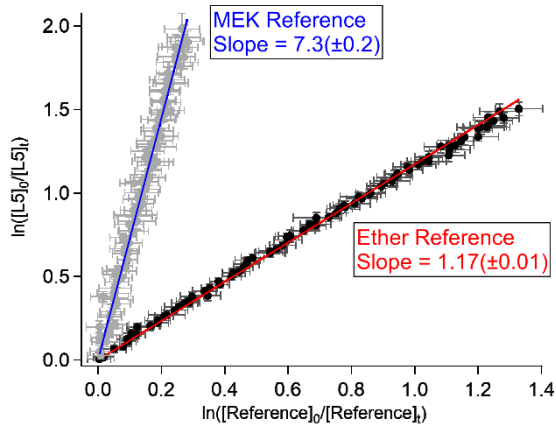
126

### 127 **3 RESULTS AND DISCUSSION**

#### 128 **3.1 Rate Constant Measurements**

129 The rate constants for VMS oxidation are determined via a relative rate analysis using equation  
130 1 (Figure 1). Linear fits are performed with a weighted least orthogonal distance regression as

131 implemented in IGOR Pro (Wavemetrics, v8.0.4.2) with the intercept forced through the origin.  
 132 The experimentally derived rate constants for the seven VMS with OH radicals and Cl atoms are  
 133 given in Tables 1 and 2. Uncertainty reported for the rates is two standard deviations of the three  
 134 repeats of the experiments. Uncertainty in the reference compound rate constants is omitted from  
 135 the error analysis. Slopes from individual experiments are listed in Tables S1 and S2.



136  
 137 **Figure 1** Plot of equation 1 for the oxidation of L5 by Cl atoms. Results using ether (black points)  
 138 and MEK (grey points) as the reference compound are shown. Error bars are one standard deviation  
 139 and are determined by propagating uncertainty from averaging 15 seconds of the signal for each  
 140 measurement.

141 **Table 1** Rate constants of VMS with the OH radical.

VMS	Slope <sup>a</sup> (MEK)	Rate <sup>b</sup> (MEK <sup>c</sup> )	Slope (Propionic Acid)	Rate (Propionic Acid <sup>d</sup> )	Slope <sup>e</sup> (VMS)	Rate (VMS <sup>f</sup> )
L2	1.09±0.09	1.2±0.1	0.9±0.1	1.1±0.1	*	*
L3	1.6±0.1	1.7±0.1	1.28±0.03	1.53±0.04	1.4±0.2	1.7±0.2
L4	2.2±0.2	2.5±0.2	1.6±0.1	1.9±0.1	1.9±0.4	2.5±0.5
L5	3.1±0.6	3.4±0.7	2.3±0.1	2.8±0.2	2.6±0.6	3.4±0.7

D3	0.78±0.08	0.9±0.1	0.56±0.01	0.67±0.02	*	*
D4	1.2±0.1	1.3±0.2	0.9 ±0.1	1.1±0.1	1.6±0.1	1.28±0.1
D5	2.0±0.2	2.2±0.2	1.5±0.2	1.8±0.2	2.6±0.2	2.1±0.2

142 <sup>a</sup>The slope corresponds to  $k_{VMS}/k_{\text{reference}}$  with the reference compound listed in parentheses in the  
 143 column header. <sup>b</sup>Rate constant units are  $\times 10^{-12} \text{ cm}^3 \text{ molec}^{-1} \text{ s}^{-1}$ . <sup>c</sup>The reference rate for the MEK +  
 144 OH reaction is  $(1.1\pm0.3) \times 10^{-12} \text{ cm}^3 \text{ molec}^{-1} \text{ s}^{-1}$ .<sup>32</sup> <sup>d</sup>The reference rate for the propionic acid + OH  
 145 reaction is  $(1.2\pm0.2) \times 10^{-12} \text{ cm}^3 \text{ molec}^{-1} \text{ s}^{-1}$ .<sup>32</sup> <sup>e</sup>Rates are not calculated for L2 and D3 using VMS  
 146 as a reference compound, as L2 and D3 were the reference compounds themselves. <sup>f</sup>The absolute  
 147 rates for the L2 + OH and D3 + OH reaction are  $(1.28\pm0.08) \times 10^{-12} \text{ cm}^3 \text{ molec}^{-1} \text{ s}^{-1}$  and  $(0.82\pm0.05)$   
 148  $\times 10^{-12} \text{ cm}^3 \text{ molec}^{-1} \text{ s}^{-1}$ , respectively.<sup>18</sup>

149 **Table 2** Rate constants of VMS with Cl atoms.

VMS	Slope <sup>a</sup> (MEK)	Rate <sup>b</sup> (MEK <sup>c</sup> )	Slope (Ether)	Rate (Ether <sup>d</sup> )
L2	4±1	1.5±0.5	0.56±0.02	1.39±0.05
L3	5±1	1.9±0.5	0.71±0.02	1.77±0.06
L4	6±1	2.3±0.5	0.83±0.05	2.1±0.1
L5	7±1	2.9±0.6	1.1±0.2	2.8±0.4
D3	1.4±0.1	0.57±0.05	0.20±0.05	0.5±0.1
D4	2.9±0.3	1.14±0.08	0.47±0.04	1.2±0.1
D5	4.5±0.6	1.8±0.2	0.72±0.07	1.8±0.2

150 <sup>a</sup>The slope corresponds to  $k_{VMS}/k_{\text{reference}}$  with the reference compound listed in parentheses in the  
 151 column header. <sup>b</sup>Rate constant units are  $\times 10^{-10} \text{ cm}^3 \text{ molec}^{-1} \text{ s}^{-1}$ . <sup>c</sup>The rate for the MEK + Cl reaction  
 152 used is  $(0.4\pm0.1) \times 10^{-10} \text{ cm}^3 \text{ molec}^{-1} \text{ s}^{-1}$ .<sup>32</sup> <sup>d</sup>The rate for the diethyl ether + Cl reaction used is  
 153  $(2.5\pm0.2) \times 10^{-10} \text{ cm}^3 \text{ molec}^{-1} \text{ s}^{-1}$ .<sup>33</sup>

154 For the OH radical oxidation experiments, a systematic difference exists between the rate  
 155 constants determined from the two reference compounds, with rate constants determined relative  
 156 to MEK ~20% faster than those based on propionic acid, suggesting an inconsistency between the  
 157 reference compounds' rate constants. Since absolute rate constants for L2, L3, D3, and D4 have  
 158 been measured by Bernard et al. (2018),<sup>18</sup> intrasiloxane relative rate determinations allow for the

159 determination of a self-consistent set of rate constants. Using the Bernard et al. (2018)<sup>18</sup> absolute  
160 rate constant for L2 (D3), we calculate rate constants for L3, L4, and L5 (D4 and D5) (Table 1).  
161 Using these intrasiloxane relative rate determinations, we find agreement to within 5% of Bernard  
162 et al.'s (2018) absolute measurements for L3 and 15% for D4.<sup>18</sup> These rate constants also agree  
163 within 5% of the rate constants determined using MEK as a reference compound suggesting a bias  
164 in the propionic acid rate constant. A possible explanation for this bias is that propionic acid can  
165 dimerize at high concentrations in the gas phase which potentially has created a bias in the reported  
166 literature rate constants.<sup>34</sup> Due to the potential bias when using propionic acid, we exclude those  
167 measurements from the rate constant determination. Taking a weighted average of the results using  
168 MEK and L2 (or D3 for the cyclic VMS), the rate constants with OH radicals are  $(1.20 \pm 0.09)$   
169  $\times 10^{-12}$ ,  $(1.7 \pm 0.1) \times 10^{-12}$ ,  $(2.5 \pm 0.2) \times 10^{-12}$ ,  $(3.4 \pm 0.6) \times 10^{-12}$ ,  $(0.77 \pm 0.05) \times 10^{-12}$ ,  $(1.3 \pm 0.1)$   
170  $\times 10^{-12}$ , and  $(2.1 \pm 0.2) \times 10^{-12}$   $\text{cm}^3 \text{ molec}^{-1} \text{ s}^{-1}$  for L2, L3, L4, L5, D3, D4, and D5 respectively.

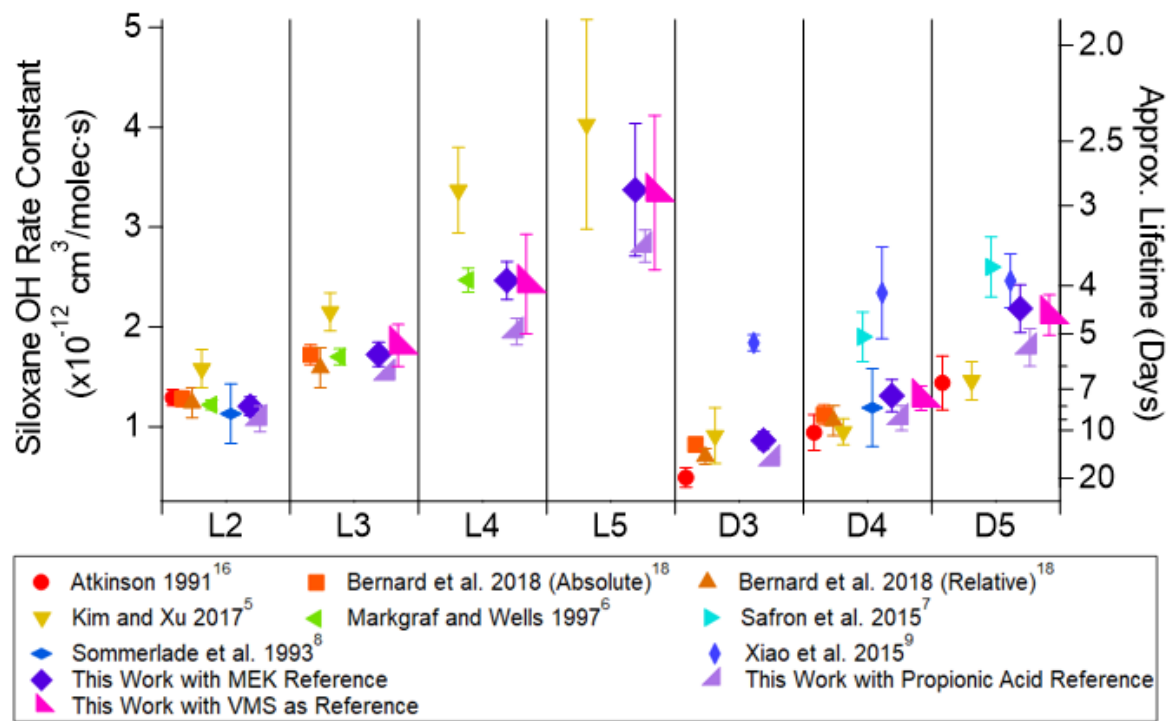
171 For Cl atom and VMS reactions, rate constants determined relative to the two reference  
172 compounds (Table 2) agree to within 20%. Rate constant uncertainty increases for the larger, faster  
173 reacting VMS as the reference compound reacts more slowly with Cl atoms, leading to larger  
174 propagated uncertainties. The weighted average rate constants for reactions with Cl atoms using  
175 ether and MEK as reference compounds with the L2, L3, L4, L5, D3, D4, and D5 are  $(1.44 \pm 0.05)$   
176  $\times 10^{-10}$ ,  $(1.85 \pm 0.05) \times 10^{-10}$ ,  $(2.2 \pm 0.1) \times 10^{-10}$ ,  $(2.9 \pm 0.1) \times 10^{-10}$ ,  $(0.56 \pm 0.05) \times 10^{-10}$ ,  $(1.16 \pm$   
177  $0.06) \times 10^{-10}$ , and  $(1.8 \pm 0.1) \times 10^{-10}$   $\text{cm}^3 \text{ molec}^{-1} \text{ s}^{-1}$ , respectively.

178

### 179 3.2 Comparison to Literature Values

180 Figure 2 compares the OH + VMS rate constants determined here to previous measurements.  
181 All literature rates were measured with the relative rate method except for Bernard et al. (2018),<sup>18</sup>

182 who made both absolute and relative measurements. Rate constants from Atkinson (1991),<sup>16</sup>  
 183 Markgraf and Wells (1997),<sup>6</sup> and Sommerlade et al. (1993)<sup>8</sup> were corrected using currently  
 184 recommended rates for the reference compounds (cyclohexane, n-hexane, and n-hexane  
 185 respectively).<sup>35</sup>



187 **Figure 2** A comparison of rate constants of VMS with OH radicals measured in this work with  
 188 MEK, propionic acid, and other VMS as reference compounds to literature reported rate  
 189 constants<sup>5-9,16,18</sup> Error bars are two standard deviations and do not include the uncertainty of the  
 190 reference compound's rate constant. The lifetime axis was calculated assuming a 24-hour average  
 191 OH concentration of  $1.2 \times 10^6$  molec cm<sup>-3</sup>.<sup>36</sup>

192 In general, rate constants in this work agree with Sommerlade et al. (1993),<sup>8</sup> Bernard et al.  
 193 (2018),<sup>18</sup> Atkinson et al. (1991),<sup>16</sup> and Markgraf and Wells (1996)<sup>6</sup> for the linear VMS, whereas  
 194 the rate constants reported by Kim and Xu (2017)<sup>5</sup> are larger. The reason for this disagreement is

195 unclear, particularly since the Kim and Xu (2017)<sup>5</sup> measurements tend to the lower end of previous  
196 measurements for the cyclic species. For the cyclic species D3 and D4, this work's measurements  
197 agree to within 15% of Bernard et al. (2018),<sup>18</sup> 25% of Kim and Xu (2017),<sup>5</sup> 3% of Sommerlad  
198 et al. (1993),<sup>8</sup> and 35% of Atkinson et al (1995),<sup>17</sup> while being lower than Xiao et al. (2015)<sup>9</sup> and  
199 Safron et al. (2015)<sup>7</sup> (D4 only). However, this work's measurement of the D5 + OH rate constant  
200 is between the four measurements from Xiao et al. (2015),<sup>9</sup> Safron et al. (2015),<sup>7</sup> Atkinson  
201 (1991),<sup>16</sup> and Kim and Xu (2017).<sup>5</sup> Disagreements in rate constants could be due to errors in  
202 reference compound rate constants or using a silicon based coating on the reaction vessel  
203 experiments were performed in,<sup>5</sup> but the exact reasons are unknown. With the additional set of rate  
204 constants determined in this work, the smaller VMS (L2, L3, D3, and D4) have multiple rate  
205 constants that agree within 20% of each other. The measured rate constants for D5 with OH  
206 radicals have more variability between studies, though the rate constant appears to be faster than  
207 previously expected.

208 To the best of our knowledge, these are the first measurements of rate constants for Cl atom  
209 oxidation of L3-L5 and D3-D5; the only other study performed on Cl atom-initiated oxidation of  
210 VMS was on L2 and its fully deuterated analog.<sup>17</sup> This work's measurement of the L2 rate constant  
211 agrees to within 10% of Atkinson et al. (1995)<sup>17</sup> measurement, as shown in Figure S2.

### 212 3.3 Structure Activity Relationship for VMS Rate Constants with OH

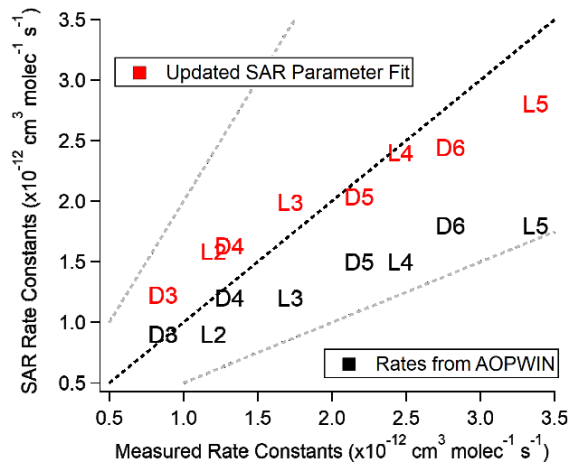
213 Structure activity relationship (SAR) models are frequently used for predicting rate constants  
214 based on the structure of the reactants. The SAR model, developed by Atkinson and co-workers<sup>37,38</sup>  
215 and based on a group-additivity relationships, is one of the most frequently used SAR models for  
216 estimating gas phase rate constants with OH radicals and it is the basis for the parameterization  
217 used in the Atmospheric Oxidation Program for Microsoft Windows (AOPWIN) module of the

218 U.S. Environmental Protection Agency's (EPA) Estimation Program Interface (EPI) Suite. Rate  
219 constants are calculated by summing the individual functional groups' contributions to the total  
220 molecule's reactivity with OH. Functional groups' individual reactivity is determined by the  
221 number and identity of substitutions adjacent to the reactive site. Since VMS oxidation is initiated  
222 through hydrogen abstraction on primary hydrogens, the rate constant of a VMS can be calculated  
223 by equation:

$$k_{OH\ Total} = \sum [k_{prim} * F(x)] \quad (2)$$

224 where  $k_{prim}$  is the contribution of a primary methyl group to OH reactivity and  $F(x)$  is the  
225 substituent factor for the group adjacent to the methyl group. In AOPWIN (v1.92), VMS + OH  
226 rate constants are estimated using a rate of H-abstraction  $k_{prim}$  of  $0.136 \times 10^{-12} \text{ cm}^3 \text{ molec}^{-1} \text{ s}^{-1}$ , with  
227 substituent factor of 1.1 corresponding to  $F(\text{Si})$ . This parameterization predicts OH radical rate  
228 constants for cyclic VMS larger than D4 that are significantly smaller than the measured rate  
229 constants, with larger systematic discrepancies for linear VMS (Figure 3). Since it has repeatedly  
230 been shown both in this work and in previous studies that linear VMS react faster than cyclic VMS  
231 with the same number of methyl groups<sup>5,6,18</sup> (Figure S3), we propose that multiple substituent  
232 factors are required. We investigated two modifications to the SAR model. The first modification  
233 treats cyclic and linear compounds separately, assigning substituent factors  $F(\text{Si}_{\text{Cyclic}})$  and  
234  $F(\text{Si}_{\text{Linear}})$ . The other modification extends the substituent factor from  $F(\text{Si})$  to  $F(-\text{Si}(\text{CH}_3)_2\text{OR})$  for  
235  $\alpha$ -Si atom in the terminal position of a linear VMS and  $F(-\text{SiCH}_3(\text{OR})_2)$  for  $\alpha$ -Si atom in the center  
236 of a linear VMS or at any position in a cyclic VMS. A comparison between the two  
237 parameterizations is provided in section 5 of the supporting information. The second  
238 parameterization more accurately predicts the rate constants and we propose a  $F(-\text{Si}(\text{CH}_3)_2\text{OR})$  of  
239 1.9 and  $F(-\text{SiCH}_3(\text{OR})_2)$  of 1.5. Rate constants calculated using these substituent factors and rate  
240

241 constants calculated by AOPWIN are shown in Figure 3. Figure S4 shows the results using  
242  $F(\text{Si}_{\text{Cyclic}})$  and  $F(\text{Si}_{\text{Linear}})$ .



243

244 **Figure 3** Plot of AOPWIN rate constants versus measured rate constants in addition to this work's  
245 SAR versus measured rate constants. Measured rate constant for D6 is from Safron et al.<sup>7</sup> The  
246 dashed black line represents a 1:1 relationship and the two dashed grey lines are 2:1 and 0.5:1.

247 Although there is improvement in the predictive capability of the SAR model when using  $F(-$   
248  $\text{SiCH}_3(\text{OR})_2)$  and  $F(-\text{Si}(\text{CH}_3)_2\text{OR})$ , the rates calculated with the revised substituent factors are still  
249 slightly low for the larger VMS and slightly high for the small VMS. Since previous quantum  
250 calculations have shown that no significant energy difference between abstraction of the hydrogens  
251 on an terminating or central methyl group exists,<sup>18</sup> it is unsurprising that this empirical SAR  
252 formulation has difficulty in reproducing measured rate constants. Bernard et al. (2018)<sup>18</sup> suggests  
253 that the possible reason linear VMS react faster than cyclic VMS with equivalent number of methyl  
254 groups is formation of an H-bonded prereactive complex with the hydroxyl radical and the O in  
255 the Si-O-Si bridge for linear VMS. This is similar to the transition state stabilization by hydrogen  
256 bonding that occurs in ether oxidation,<sup>39</sup> another class of compounds that empirical SAR

257 formulations have struggled to represent. Further experimental and theoretical investigation is  
258 needed to understand the differences between the linear and cyclic VMS reactivity.

259 3.4 Reaction Products

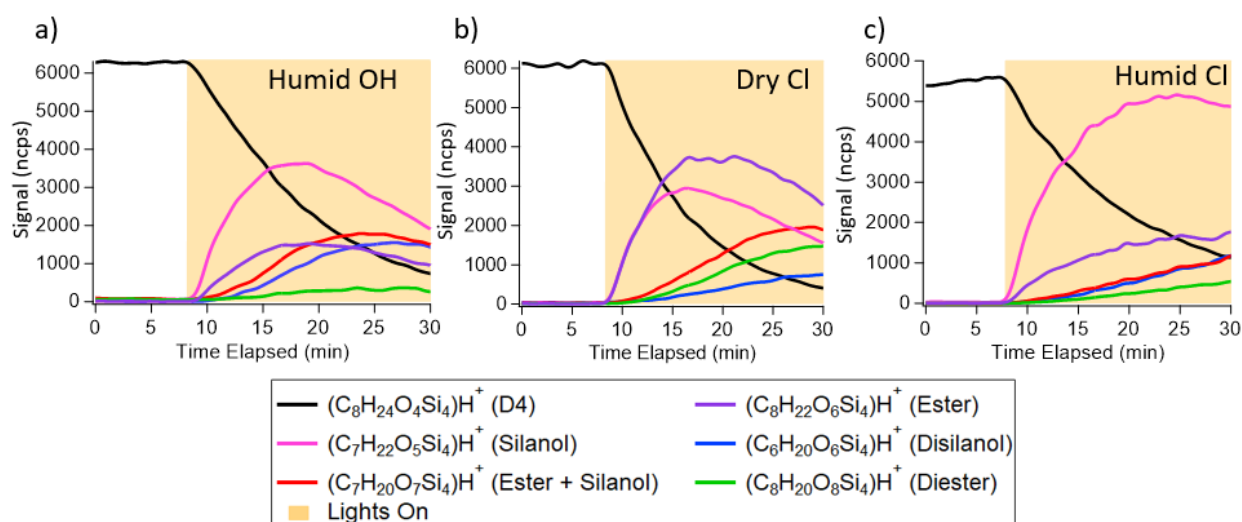
260 Both OH radicals and Cl atoms initiate oxidation through hydrogen abstraction from a methyl  
261 group, forming a substituted-alkyl radical which quickly reacts with ambient oxygen to form a  
262 peroxy radical. Subsequent reactions of the peroxy radical are uncertain. Although formation of a  
263 silanol ( $\text{Si}(\text{OR})_2(\text{CH}_3)(\text{OH})$ ; replacement of a methyl group by a hydroxyl group) is generally  
264 regarded as the first stable oxidation product,<sup>6,17,22</sup> it has been suggested that the first generation  
265 product is a formate ester with the formula  $\text{Si}(\text{OR})_2(\text{CH}_3)(\text{OC(O)H})$  which then hydrolyzes to form  
266 the silanol.<sup>17</sup> Other groups have not directly identified the ester product, potentially because many  
267 previous measurements have required collection onto a substrate before analysis and it is likely  
268 that the ester reacts or decomposes on the substrate. There has been an alternate suggestion that an  
269 early generation product is a silyl methanol with a formula of  $\text{Si}(\text{OR})_2(\text{CH}_3)(\text{CH}_2\text{OH})$ .<sup>8,22</sup>  
270 Dimerization of VMS have also been seen in the particle and gas phases, with the bridge between  
271 the two VMS either an oxygen atom,  $\text{CH}_2$ , or  $\text{CH}_2\text{CH}_2$ .<sup>8,22</sup> Structures for the ester, silanol, and silyl  
272 methanol formulas are shown in Figure S5.

273 To investigate the oxidation products of VMS, D4 oxidation experiments were performed with  
274 no other VMS or relative rate tracer present in the chamber. We expect similar oxidation products  
275 for all cyclic VMS. In general, oxidation by OH radicals and Cl atoms yielded the same oxidation  
276 products with the two main first generation products detected having formulas of  $\text{C}_8\text{H}_{22}\text{O}_6\text{Si}_4\text{H}^+$   
277 and  $\text{C}_7\text{H}_{22}\text{O}_5\text{Si}_4\text{H}^+$ . These formulas are consistent with the protonated ester and silanol products,  
278 respectively. As the instrumentation used in these experiments can only determine molecular  
279 formulas based on the mass-to-charge of a detected species, isomeric interpretation of assigned

280 molecular formulas is based on previous studies.<sup>6,17</sup> Previous measurements<sup>6,17</sup> have reported a  
281 delay in the rise of the silanol product, leading to the suggestion that the silanol was formed from  
282 the hydrolysis of the ester. However, our work showed a near simultaneous increase in both  
283 products (Figure 4). Possible explanations for these results include differences in peroxy radical  
284 fates between studies or chemistry occurring on the walls of the chamber producing the silanol  
285 faster than through gas phase hydrolysis. Wall partitioning could be an important process occurring  
286 preferentially with the oxidation products over the parent VMS, changing the observed gas phase  
287 oxidation products. The vapor pressure of D5 is 0.204 mbar (a mass saturation concentration, C\*,  
288 of  $3 \times 10^6 \text{ ug m}^{-3}$ ),<sup>40</sup> while adding an ester functional group is estimated to lower the vapor pressure  
289 by approximately one order of magnitude to 0.013 mbar (C\* of  $2.1 \times 10^5 \text{ ug m}^{-3}$ ).<sup>41</sup> Using these  
290 vapor pressures and assuming the chamber walls contribute a C<sub>w</sub> of  $10 \text{ mg m}^{-3}$ ,<sup>42</sup> less than 0.5%  
291 of the D5 is expected to partition onto the walls while 5% of the ester product could partition to  
292 the walls. If the hydrolysis of the ester is a surface mediated reaction, then different surface area  
293 to volume ratios of experimental setups will change the temporal evolution of the products.  
294 Additionally, we find no evidence for the silyl methanol ( $\text{Si}(\text{OR})_2(\text{CH}_3)(\text{CH}_2\text{OH})$ ) product or  
295 dimer formation from oxidized VMS. To better understand the oxidation mechanism of VMS,  
296 future investigations should include varying the fate and lifetime of the initially formed peroxy  
297 radical and careful consideration of the wall processes.

298 Other oxidation products observed include compounds indicative of multigenerational chemistry  
299 such as disilanols or compounds with one ester group and one silanol group on a VMS (Figure 4).  
300 As multigenerational products have the same functional groups as the first-generation products,  
301 further oxidation must be initiated by hydrogen abstraction from the remaining methyl groups.

302     Although the same product ions are present in both the Cl atom and OH radical oxidation  
 303    experiments, the relative intensity of the ions depends on the oxidant identity. In experiments with  
 304    OH radicals as the oxidant, the intensity of the ester is suppressed and the intensity of the silanol  
 305    product is enhanced compared to the Cl atom experiments. Given that hydrolysis reactions have  
 306    been hypothesized to be important, a possible explanation is differences in water content between  
 307    the two experiments. In the standard experiments, water is added to the chamber (~20% RH) in  
 308    order to form OH radicals, while Cl atom oxidation occurs under dry conditions. To investigate if  
 309    the presence of water could explain the product ion differences, D4 oxidation with Cl atoms was  
 310    repeated under humid (~20% RH) conditions (Figure 4). These experiments showed an enhanced  
 311    silanol and suppressed ester signal suggesting that humidity effects were at least partly responsible  
 312    for the differences in the formed products. The relative intensities of the silanol and ester products  
 313    compared to the parent D4 are not the same between the humid Cl atom and OH radical oxidation  
 314    experiments, implying that there is different peroxy radical chemistry or chamber wall interactions  
 315    that can affect the oxidation mechanism. Despite the product ion intensity differences between Cl  
 316    atom and OH radical oxidation experiments, both oxidants generally form the same products.



318 **Figure 4** Time-series of oxidation products of D4 (black trace) with (a) OH Radicals and ~20%  
319 RH, (b) Cl atoms in dry (<2% RH) conditions, and (c) Cl atoms in humid (~20% RH) conditions.  
320 Signals are normalized to the toluene reagent ion and smoothed.

321 3.5 Global VMS Atmospheric Lifetime

322 Table 3 compares the average atmospheric lifetimes for the VMS investigated here using an  
323 estimated global average concentration of OH radicals ( $1.2 \times 10^6$  molec  $\text{cm}^{-3}$ )<sup>36</sup> and Cl atoms (620  
324 molec  $\text{cm}^{-3}$ )<sup>43</sup> with the rate constants measured in this work. These values assume a rate constant  
325 at 297 K, which is higher than the tropospheric average and thus leads to calculated lifetimes that  
326 are biased low. While OH radical oxidation accounts for the majority of the VMS loss, Cl atoms  
327 contribute a few percent to the total removal of the VMS in the atmosphere.

328 **Table 3** Estimated atmospheric lifetimes of VMS and percent loss due to Cl atom oxidation.

VMS	Global OH and Global Cl <sup>a</sup>	
	Lifetime (Days)	% Loss Due to Cl atoms
L2	7.6	5.8
L3	5.4	5.3
L4	3.7	4.3
L5	2.7	4.2
D3	11	3.3
D4	7.1	4.4
D5	4.4	4.2

329 <sup>a</sup>Values were calculated assuming a global 24 hour average concentration of OH radicals of  $1.2 \times 10^6$  molec  $\text{cm}^{-3}$ <sup>36</sup> and 620 molec  $\text{cm}^{-3}$  of Cl atoms.<sup>43</sup>

331 Knowledge of the global lifetime of VMS is important to understand the average lifetime of  
332 VMS but global averages fail to capture local air chemistry which could have significantly

333 different oxidant concentrations. Measurements over approximately the last decade have found  
334 that Cl atom chemistry plays a more significant role in the oxidation capacity of polluted  
335 atmospheres than traditionally thought. In polluted environments, Cl atom concentration peaks in  
336 the morning due to the photolysis of nocturnal reservoirs such as  $\text{ClNO}_2$ .<sup>26,44-47</sup> Although  
337 knowledge of the temporal variation of VMS concentrations is sparse, particularly the variation on  
338 a diurnal timescale, a recent study suggests that VMS concentrations peak in the morning due to  
339 emissions from personal care product use.<sup>48</sup> Due to this potential temporal overlap, the Cl atom-  
340 initiated oxidation may be more important in determining urban VMS chemistry than the global  
341 averages suggest. Using a temporal profile of the Cl atom to OH radical ratio measured during the  
342 CalNex 2010 campaign<sup>49</sup> and D5 measured in Boulder, CO, USA and Toronto, ON, Canada, we  
343 estimate that Cl accounts for 25-30% of the D5 oxidation that occurs by noon. Details of this  
344 calculation are provided in section 7 of the supporting information (Figures S6-S7). This chlorine  
345 initiated chemistry may have important implications for urban air quality since VMS oxidation has  
346 been suggested as a source of the Si observed in urban ultrafine aerosol.<sup>10</sup>

347 The results presented here suggest that while the influence of Cl atoms on global VMS lifetime  
348 is small, Cl atom chemistry may have a larger impact in polluted urban environments particularly  
349 with regard to the production of oxidized VMS. As the chemistry of oxidized VMS and their  
350 impacts on the environment are poorly understood, further work on VMS oxidation products is  
351 required in order to have a complete understanding of VMS environmental fate and contribution  
352 to urban air quality.

353

354

355

356 ASSOCIATED CONTENT

357 **Supporting Information.**

358 The following files are available free of charge.

359 Detailed information of the mass spectrometer used, individual experiment's results, comparison  
360 of relative rate data to literature values, the structure-activity relationship for estimating the OH  
361 rate constants with VMS, proposed structures of VMS oxidation products, and impact of Cl atoms  
362 in urban environments (PDF)

363 AUTHOR INFORMATION

364 Corresponding Author

365 \*Eleanor.Browne@Colorado.edu, 303-735-7685, ORCID iD 0000-0002-8076-9455

366 Authors

367 Mitchell Alton ORCID iD 0000-0002-7119-3706

368 ACKNOWLEDGMENT

369 This research was supported by the National Science Foundation under Grant CHE-1808606. We  
370 thank Paul Ziemann for helpful discussions.

371

372

373

374

## 375 REFERENCES

376 (1) Brooke, D.; Crookes, M.; Gray, D.; Robertson, S. *Environmental Risk Assessment Report: 377 Decamethylcyclopentasiloxane*; Environment Agency, 2009.

378 (2) Genualdi, S.; Harner, T.; Cheng, Y.; MacLeod, M.; Hansen, K. M.; Van Egmond, R.; 379 Shoeib, M.; Lee, S. C. Global Distribution of Linear and Cyclic Volatile Methyl Siloxanes 380 in Air. *Environ. Sci. Technol.* **2011**, *45* (8), 3349–3354. <https://doi.org/10.1021/es200301j>.

381 (3) Allen, R. B.; Annelin, R. B.; Atkinson, R.; Carpenter, J. C.; Carter, W. L. P.; Chandra, G.; 382 Fendinger, N. J.; Gerhards, R.; Grigoras, S.; Hatcher, J. A.; Hobson, J. F.; Kochs, P.; 383 Lehmann, R. G.; Maxim, L. D.; Mazzoni, S. M.; Mihaich, E. M.; Miyakawa, Y.; Pohl, E. 384 R.; Powell, D. E.; Roy, S.; Sawano, T.; Slater, G. S.; Spivack, J. L.; Stevens, C.; Wischer, 385 D. *Organosilicon Materials*; Chandra, G., Ed.; The Handbook of Environmental Chemistry; 386 Springer Berlin Heidelberg: Berlin, Heidelberg, 1997; Vol. 3. <https://doi.org/10.1007/978-3-540-68331-5>.

388 (4) Germain, P.; Thomas, K.; Noguchi, T. Silicone Research - An Industry Commitment 389 [https://www.cyclosiloxanes.org/uploads/Modules/Links/silicone-research\\_an-industry- commitment.pdf](https://www.cyclosiloxanes.org/uploads/Modules/Links/silicone-research_an-industry- 390 commitment.pdf) (accessed Dec 6, 2019).

391 (5) Kim, J.; Xu, S. Quantitative Structure-Reactivity Relationships of Hydroxyl Radical Rate 392 Constants for Linear and Cyclic Volatile Methylsiloxanes. *Environ. Toxicol. Chem.* **2017**, 393 *36* (12), 3240–3245. <https://doi.org/10.1002/etc.3914>.

394 (6) Markgraf, S. J.; Wells, J. R. The Hydroxyl Radical Reaction Rate Constants and 395 Atmospheric Reaction Products of Three Siloxanes. *Int. J. Chem. Kinet.* **1997**, *29* (6), 445–

396 451. [https://doi.org/10.1002/\(SICI\)1097-4601\(1997\)29:6<445::AID-KIN6>3.0.CO;2-U](https://doi.org/10.1002/(SICI)1097-4601(1997)29:6<445::AID-KIN6>3.0.CO;2-U).

397 (7) Safron, A.; Strandell, M.; Kierkegaard, A.; Macleod, M. Rate Constants and Activation  
398 Energies for Gas-Phase Reactions of Three Cyclic Volatile Methyl Siloxanes with the  
399 Hydroxyl Radical. *Int. J. Chem. Kinet.* **2015**, *47* (7), 420–428.  
400 <https://doi.org/10.1002/kin.20919>.

401 (8) Sommerlade, R.; Parlar, H.; Wrobel, D.; Kochs, P. Product Analysis and Kinetics of the  
402 Gas-Phase Reactions of Selected Organosilicon Compounds with OH Radicals Using a  
403 Smog Chamber-Mass Spectrometer System. *Environ. Sci. Technol.* **1993**, *27* (12), 2435–  
404 2440. <https://doi.org/10.1021/es00048a019>.

405 (9) Xiao, R.; Zammit, I.; Wei, Z.; Hu, W.-P.; MacLeod, M.; Spinney, R. Kinetics and  
406 Mechanism of the Oxidation of Cyclic Methylsiloxanes by Hydroxyl Radical in the Gas  
407 Phase: An Experimental and Theoretical Study. *Environ. Sci. Technol.* **2015**, *49* (22),  
408 13322–13330. <https://doi.org/10.1021/acs.est.5b03744>.

409 (10) Bzdek, B. R.; Horan, A. J.; Pennington, M. R.; Janechek, N. J.; Baek, J.; Stanier, C. O.;  
410 Johnston, M. V. Silicon Is a Frequent Component of Atmospheric Nanoparticles. *Environ.*  
411 *Sci. Technol.* **2014**, *48* (19), 11137–11145. <https://doi.org/10.1021/es5026933>.

412 (11) Wu, Y.; Johnston, M. V. Aerosol Formation from OH Oxidation of the Volatile Cyclic  
413 Methyl Siloxane (CVMS) Decamethylcyclopentasiloxane. *Environ. Sci. Technol.* **2017**, *51*  
414 (8), 4445–4451. <https://doi.org/10.1021/acs.est.7b00655>.

415 (12) Brooke, D. N.; Brooke, M. J.; Gray, D.; Robertson, S.; Crookes, M.; Gray, D.; Robertson,  
416 S. *Environmental Risk Assessment Report: Octamethylcyclotetrasiloxane*; Environment

417 Agency, 2009.

418 (13) Xu, S.; Warner, N.; Bohlin-Nizzetto, P.; Durham, J.; McNett, D. Long-Range Transport  
419 Potential and Atmospheric Persistence of Cyclic Volatile Methylsiloxanes Based on Global  
420 Measurements. *Chemosphere* **2019**, 228, 460–468.  
421 <https://doi.org/10.1016/j.chemosphere.2019.04.130>.

422 (14) Janechek, N. J.; Hansen, K. M.; Stanier, C. O. Comprehensive Atmospheric Modeling of  
423 Reactive Cyclic Siloxanes and Their Oxidation Products. *Atmos. Chem. Phys.* **2017**, 17 (13),  
424 8357–8370. <https://doi.org/10.5194/acp-17-8357-2017>.

425 (15) Mackay, D.; Cowan-Ellsberry, C. E.; Powell, D. E.; Woodburn, K. B.; Xu, S.; Kozerski, G.  
426 E.; Kim, J. Decamethylcyclopentasiloxane (D5) Environmental Sources, Fate, Transport,  
427 and Routes of Exposure. *Environ. Toxicol. Chem.* **2015**, 34 (12), 2689–2702.  
428 <https://doi.org/10.1002/etc.2941>.

429 (16) Atkinson, R. Kinetics of the Gas-Phase Reactions of a Series of Organosilicon Compounds  
430 with Hydroxyl and Nitrate (NO<sub>3</sub>) Radicals and Ozone at 297 +/- 2 K. *Environ. Sci. Technol.*  
431 **1991**, 25 (5), 863–866. <https://doi.org/10.1021/es00017a005>.

432 (17) Atkinson, R.; Tuazon, E. C.; Kwok, E. S. C.; Arey, J.; Aschmann, S. M.; Bridier, I. Kinetics  
433 and Products of the Gas-Phase Reactions of (CH<sub>3</sub>)<sub>4</sub>Si, (CH<sub>3</sub>)<sub>3</sub>SiCH<sub>2</sub>OH,  
434 (CH<sub>3</sub>)<sub>3</sub>SiOSi(CH<sub>3</sub>)<sub>3</sub> and (CD<sub>3</sub>)<sub>3</sub>SiOSi(CD<sub>3</sub>)<sub>3</sub> with Cl Atoms and OH Radicals. *J. Chem.*  
435 *Soc. Faraday Trans.* **1995**, 91 (18), 3033. <https://doi.org/10.1039/ft9959103033>.

436 (18) Bernard, F.; Papanastasiou, D. K.; Papadimitriou, V. C.; Burkholder, J. B. Temperature  
437 Dependent Rate Coefficients for the Gas-Phase Reaction of the OH Radical with Linear

438 (L2, L3) and Cyclic (D3 , D4) Permethylsiloxanes. *J. Phys. Chem. A* **2018**, *122* (17), 4252–  
439 4264. <https://doi.org/10.1021/acs.jpca.8b01908>.

440 (19) McLachlan, M. S.; Kierkegaard, A.; Hansen, K. M.; Van Egmond, R.; Christensen, J. H.;  
441 Skjøth, C. A. Concentrations and Fate of Decamethylcyclopentasiloxane (D5) in the  
442 Atmosphere. *Environ. Sci. Technol.* **2010**, *44* (14), 5365–5370.  
443 <https://doi.org/10.1021/es100411w>.

444 (20) Buser, A. M.; Kierkegaard, A.; Bogdal, C.; Macleod, M.; Scheringer, M.; Hungerbühler, K.  
445 Concentrations in Ambient Air and Emissions of Cyclic Volatile Methylsiloxanes in Zurich,  
446 Switzerland. *Environ. Sci. Technol.* **2013**, *47* (13), 7045–7051.  
447 <https://doi.org/10.1021/es3046586>.

448 (21) Buser, A. M.; Bogdal, C.; MacLeod, M.; Scheringer, M. Emissions of  
449 Decamethylcyclopentasiloxane from Chicago. *Chemosphere* **2014**, *107*, 473–475.  
450 <https://doi.org/10.1016/j.chemosphere.2013.12.034>.

451 (22) Wu, Y.; Johnston, M. V. Molecular Characterization of Secondary Aerosol from Oxidation  
452 of Cyclic Methylsiloxanes. *J. Am. Soc. Mass Spectrom.* **2016**, *27* (3), 402–409.  
453 <https://doi.org/10.1007/s13361-015-1300-1>.

454 (23) Janecek, N. J.; Marek, R. F.; Bryngelson, N.; Singh, A.; Bullard, R. L.; Brune, W. H.;  
455 Stanier, C. O. Physical Properties of Secondary Photochemical Aerosol from OH Oxidation  
456 of a Cyclic Siloxane. *Atmos. Chem. Phys.* **2019**, *19* (3), 1649–1664.  
457 <https://doi.org/10.5194/acp-19-1649-2019>.

458 (24) Faxon, C. B.; Bean, J. K.; Ruiz, L. H. Inland Concentrations of Cl<sub>2</sub> and ClNO<sub>2</sub> in Southeast

459 Texas Suggest Chlorine Chemistry Significantly Contributes to Atmospheric Reactivity.

460 *Atmosphere (Basel)*. **2015**, *6* (10), 1487–1506. <https://doi.org/10.3390/atmos6101487>.

461 (25) Faxon, C. B.; Allen, D. T. Chlorine Chemistry in Urban Atmospheres: A Review. *Environ.*  
462 *Chem.* **2013**, *10* (3), 221–233. <https://doi.org/10.1071/EN13026>.

463 (26) Thornton, J. A.; Kercher, J. P.; Riedel, T. P.; Wagner, N. L.; Cozic, J.; Holloway, J. S.; Dub,  
464 W. P.; Wolfe, G. M.; Quinn, P. K.; Middlebrook, A. M.; Alexander, B.; Brown, S. S. A  
465 Large Atomic Chlorine Source Inferred from Mid-Continental Reactive Nitrogen  
466 Chemistry. *Nature* **2010**, *464* (7286), 271–274. <https://doi.org/10.1038/nature08905>.

467 (27) Ahrens, L.; Harner, T.; Shoeib, M. Temporal Variations of Cyclic and Linear Volatile  
468 Methylsiloxanes in the Atmosphere Using Passive Samplers and High-Volume Air  
469 Samplers. *Environ. Sci. Technol.* **2014**, *48* (16), 9374–9381.  
470 <https://doi.org/10.1021/es502081j>.

471 (28) Gallego, E.; Perales, J. F.; Roca, F. J.; Guardino, X.; Gadea, E. Volatile Methyl Siloxanes  
472 (VMS) Concentrations in Outdoor Air of Several Catalan Urban Areas. *Atmos. Environ.*  
473 **2017**, *155*, 108–118. <https://doi.org/10.1016/j.atmosenv.2017.02.013>.

474 (29) Tran, T. M.; Abualnaja, K. O.; Asimakopoulos, A. G.; Covaci, A.; Gevao, B.; Johnson-  
475 Restrepo, B.; Kumosani, T. A.; Malarvannan, G.; Minh, T. B.; Moon, H. B.; Nakata, H.;  
476 Sinha, R. K.; Kannan, K. A Survey of Cyclic and Linear Siloxanes in Indoor Dust and Their  
477 Implications for Human Exposures in Twelve Countries. *Environ. Int.* **2015**, *78*, 39–44.  
478 <https://doi.org/10.1016/j.envint.2015.02.011>.

479 (30) Kim, Y. H.; Kim, S. Improved Abundance Sensitivity of Molecular Ions in Positive-Ion

480                   APCI MS Analysis of Petroleum in Toluene. *J. Am. Soc. Mass Spectrom.* **2010**, *21* (3), 386–  
481                   392. <https://doi.org/10.1016/j.jasms.2009.11.001>.

482                   (31) Finlayson-Pitts, B. J.; Pitts, J. N. Kinetics and Atmospheric Chemistry. *Chem. Up. Low.*  
483                   *Atmos.* **2000**, 130–178. <https://doi.org/10.1016/b978-012257060-5/50007-1>.

484                   (32) Atkinson, R.; Baulch, D. L.; Cox, R. A.; Crowley, J. N.; Hampson, R. F.; Hynes, R. G.;  
485                   Jenkin, M. E.; Rossi, M. J.; Troe, J. IUPAC Task Group on Atmospheric Chemical Kinetic  
486                   Data Evaluation, <Http://Iupac.Pole-Ether.Fr>. *Atmos. Chem. Phys.* **2004**, *4* (6), 1461–1738.  
487                   <https://doi.org/10.5194/acp-4-1461-2004>.

488                   (33) Nelson, L.; Rattigan, O.; Neavyn, R.; Sidebottom, H.; Treacy, J.; Nielsen, O. J. Absolute  
489                   and Relative Rate Constants for the Reactions of Hydroxyl Radicals and Chlorine Atoms  
490                   with a Series of Aliphatic Alcohols and Ethers at 298 K. *Int. J. Chem. Kinet.* **1990**, *22* (11),  
491                   1111–1126. <https://doi.org/10.1002/kin.550221102>.

492                   (34) Wallington, T. J.; Dagaut, P.; Liu, R.; Kurylo, M. J. The Gas Phase Reactions of Hydroxyl  
493                   Radicals with a Series of Esters over the Temperature Range 240–440 K. *Int. J. Chem.*  
494                   *Kinet.* **1988**, *20* (2), 177–186. <https://doi.org/10.1002/kin.550200210>.

495                   (35) Atkinson, R. Kinetics of the Gas-Phase Reactions of OH Radicals with Alkanes and  
496                   Cycloalkanes. *Atmos. Chem. Phys.* **2003**, *3* (6), 2233–2307. <https://doi.org/10.5194/acp-3-2233-2003>.

498                   (36) Lelieveld, J.; Gromov, S.; Pozzer, A.; Taraborrelli, D. Global Tropospheric Hydroxyl  
499                   Distribution, Budget and Reactivity. *Atmos. Chem. Phys.* **2016**, *16* (19), 12477–12493.  
500                   <https://doi.org/10.5194/acp-16-12477-2016>.

501 (37) Atkinson, R. A Structure-activity Relationship for the Estimation of Rate Constants for the  
502 Gas-phase Reactions of OH Radicals with Organic Compounds. *Int. J. Chem. Kinet.* **1987**,  
503 *19* (9), 799–828. <https://doi.org/10.1002/kin.550190903>.

504 (38) Kwok, E. S. C.; Atkinson, R. Estimation of Hydroxyl Radical Reaction Rate Constants for  
505 Gas-Phase Organic Compounds Using a Structure-Reactivity Relationship: An Update.  
506 *Atmos. Environ.* **1995**, *29* (14), 1685–1695. [https://doi.org/10.1016/1352-2310\(95\)00069-B](https://doi.org/10.1016/1352-2310(95)00069-B).

508 (39) Porter, E.; Wenger, J.; Treacy, J.; Sidebottom, H.; Mellouki, A.; Téton, S.; LeBras, G.  
509 Kinetic Studies on the Reactions of Hydroxyl Radicals with Diethers and Hydroxyethers. *J.*  
510 *Phys. Chem. A* **1997**, *101* (32), 5770–5775. <https://doi.org/10.1021/jp971254i>.

511 (40) Lei, Y. D.; Wania, F.; Mathers, D. Temperature-Dependent Vapor Pressure of Selected  
512 Cyclic and Linear Polydimethylsiloxane Oligomers. *J. Chem. Eng. Data* **2010**, *55* (12),  
513 5868–5873. <https://doi.org/10.1021/je100835n>.

514 (41) Pankow, J. F.; Asher, W. E. SIMPOL.1: A Simple Group Contribution Method for  
515 Predicting Vapor Pressures and Enthalpies of Vaporization of Multifunctional Organic  
516 Compounds. *Atmos. Chem. Phys.* **2008**, *8* (10), 2773–2796. <https://doi.org/10.5194/acp-8-2773-2008>.

518 (42) Zhang, X.; Cappa, C. D.; Jathar, S. H.; McVay, R. C.; Ensberg, J. J.; Kleeman, M. J.;  
519 Seinfeld, J. H. Influence of Vapor Wall Loss in Laboratory Chambers on Yields of  
520 Secondary Organic Aerosol. *Proc. Natl. Acad. Sci. U. S. A.* **2014**, *111* (16), 5802–5807.  
521 <https://doi.org/10.1073/pnas.1404727111>.

522 (43) Wang, X.; Jacob, D. J.; Eastham, S. D.; Sulprizio, M. P.; Zhu, L.; Chen, Q.; Alexander, B.;  
523 Sherwen, T.; Evans, M. J.; Lee, B. H.; Haskins, J. D.; Lopez-Hilfiker, F. D.; Thornton, J.  
524 A.; Huey, G. L.; Liao, H. The Role of Chlorine in Global Tropospheric Chemistry. *Atmos.*  
525 *Chem. Phys.* **2019**, *19* (6), 3981–4003. <https://doi.org/10.5194/acp-19-3981-2019>.

526 (44) Osthoff, H. D.; Roberts, J. M.; Ravishankara, A. R.; Williams, E. J.; Lerner, B. M.;  
527 Sommariva, R.; Bates, T. S.; Coffman, D.; Quinn, P. K.; Dibb, J. E.; Stark, H.; Burkholder,  
528 J. B.; Talukdar, R. K.; Meagher, J.; Fehsenfeld, F. C.; Brown, S. S. High Levels of Nitryl  
529 Chloride in the Polluted Subtropical Marine Boundary Layer. *Nat. Geosci.* **2008**, *1* (5), 324–  
530 328. <https://doi.org/10.1038/ngeo177>.

531 (45) Baker, A. K.; Sauvage, C.; Thorenz, U. R.; van Velthoven, P.; Oram, D. E.; Zahn, A.;  
532 Brenninkmeijer, C. A. M.; Williams, J. Evidence for Strong, Widespread Chlorine Radical  
533 Chemistry Associated with Pollution Outflow from Continental Asia. *Sci. Rep.* **2016**, *6* (1),  
534 36821. <https://doi.org/10.1038/srep36821>.

535 (46) Riedel, T. P.; Bertram, T. H.; Crisp, T. A.; Williams, E. J.; Lerner, B. M.; Vlasenko, A.; Li,  
536 S. M.; Gilman, J.; De Gouw, J.; Bon, D. M.; Wagner, N. L.; Brown, S. S.; Thornton, J. A.  
537 Nitryl Chloride and Molecular Chlorine in the Coastal Marine Boundary Layer. *Environ.*  
538 *Sci. Technol.* **2012**, *46* (19), 10463–10470. <https://doi.org/10.1021/es204632r>.

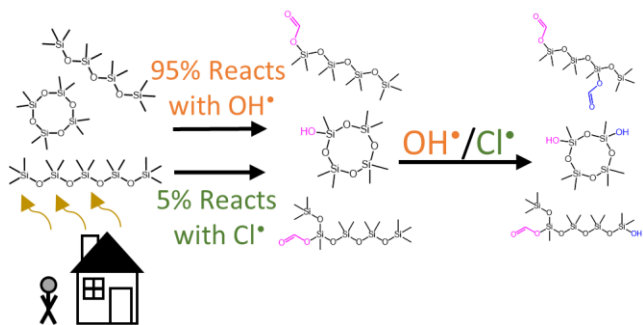
539 (47) Le Breton, M.; Hallquist, Å. M.; Kant Pathak, R.; Simpson, D.; Wang, Y.; Johansson, J.;  
540 Zheng, J.; Yang, Y.; Shang, D.; Wang, H.; Liu, Q.; Chan, C.; Wang, T.; Bannan, T. J.;  
541 Priestley, M.; Percival, C. J.; Shallcross, D. E.; Lu, K.; Guo, S.; Hu, M.; Hallquist, M.  
542 Chlorine Oxidation of VOCs at a Semi-Rural Site in Beijing: Significant Chlorine  
543 Liberation from ClNO<sub>2</sub> and Subsequent Gas- A Nd Particle-Phase Cl-VOC Production.

544 *Atmos. Chem. Phys.* **2018**, *18* (17), 13013–13030. <https://doi.org/10.5194/acp-18-13013-2018>.

546 (48) Coggon, M. M.; McDonald, B. C.; Vlasenko, A.; Veres, P. R.; Bernard, F.; Koss, A. R.;  
547 Yuan, B.; Gilman, J. B.; Peischl, J.; Aikin, K. C.; DuRant, J.; Warneke, C.; Li, S.; de Gouw,  
548 J. A. Diurnal Variability and Emission Pattern of Decamethylcyclopentasiloxane (D5) from  
549 the Application of Personal Care Products in Two North American Cities. *Environ. Sci.  
550 Technol.* **2018**, *52* (10), 5610–5618. <https://doi.org/10.1021/acs.est.8b00506>.

551 (49) Young, C. J.; Washenfelder, R. A.; Edwards, P. M.; Parrish, D. D.; Gilman, J. B.; Kuster,  
552 W. C.; Mielke, L. H.; Osthoff, H. D.; Tsai, C.; Pikelnaya, O.; Stutz, J.; Veres, P. R.; Roberts,  
553 J. M.; Griffith, S.; Dusanter, S.; Stevens, P. S.; Flynn, J.; Grossberg, N.; Lefer, B.;  
554 Holloway, J. S.; Peischl, J.; Ryerson, T. B.; Atlas, E. L.; Blake, D. R.; Brown, S. S. Chlorine  
555 as a Primary Radical: Evaluation of Methods to Understand Its Role in Initiation of  
556 Oxidative Cycles. *Atmos. Chem. Phys.* **2014**, *14* (7), 3427–3440.  
557 <https://doi.org/10.5194/acp-14-3427-2014>.

## TOC/Abstract Art



Supporting information for:

**Atmospheric chemistry of volatile methyl siloxanes: Kinetics and products of oxidation by OH radicals and Cl atoms**

Mitchell W. Alton<sup>1</sup>, Eleanor C. Browne<sup>1</sup>

<sup>1</sup>Department of Chemistry and Cooperative Institute for Research in Environmental Sciences, University of Colorado, Boulder, Colorado, 80309, United States

**Corresponding author:**

Eleanor Browne

University of Colorado; UCB 215, Boulder, CO 80309

Eleanor.Browne@colorado.edu

This file includes:

12 Pages  
7 Figures  
2 Tables  
References

## 1. Structures of Linear and Cyclic VMS Used

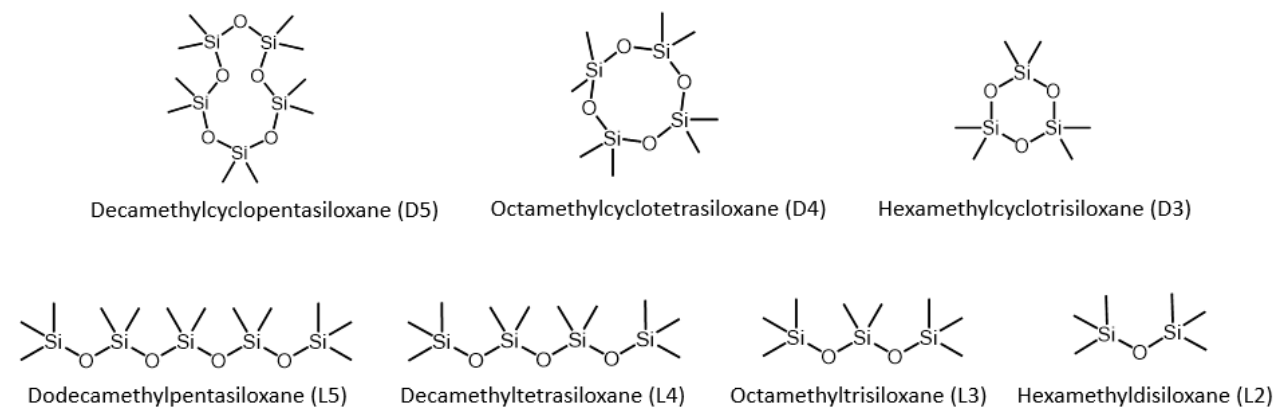


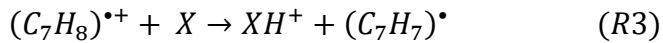
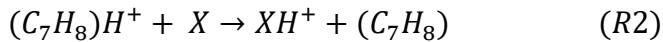
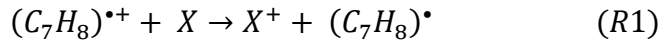
**Figure S1:** Structures of Cyclic and Linear VMS in this Work

## 2. Toluene Chemical Ionization Mass Spectrometry

A chemical ionization time-of-flight mass spectrometer was used to measure the gas-phase signals of the VMS and the reference compounds during oxidation. The reagent ion is generated by passing dry N<sub>2</sub> through the headspace of a toluene reservoir and subsequently through a Po-210 radioactive source (NRD, P-2021). Ionized toluene mixes with the gas-phase sample in the ion-molecule reactor. The sample sequentially travels through three differentially pumped regions with two radiofrequency-only quadrupoles and an ion lens stack to guide and focus the ions. The ions are orthogonally extracted into an electric field-free time-of-flight region with a reflectron. Ions are detected with a microchannel plate. Post-processing was performed in Tofware v3.2.0 (Aerodyne Research Inc.; Tofwerk AG) in Igor Pro (Wavemetrics, v8.0.4.2).

In our instrument, when sampling humid air (~20% RH) the largest signal (80% of the total reagent ion) seen in the mass spectra is the toluene ion (C<sub>7</sub>H<sub>8</sub><sup>+</sup>), with lesser contributions from C<sub>7</sub>H<sub>7</sub><sup>+</sup> (6%), C<sub>7</sub>H<sub>9</sub><sup>+</sup> (10%), C<sub>14</sub>H<sub>15</sub><sup>+</sup> (3%), and C<sub>14</sub>H<sub>16</sub><sup>+</sup> (1%). Toluene was chosen in these studies due to the lower toxicity of toluene compared to benzene.

In atmospheric pressure chemical ionization (APCI), toluene ions have been suggested to react with neutral analytes via charge transfer (Reaction R1) or proton transfer (Reactions R2 - 3).<sup>1</sup>



The ability of an analyte molecule to be ionized by charge transfer or proton transfer is determined by how the ionization energies (IE) or proton affinities (PA) of an analyte molecule and toluene compare. Charge transfer will occur when the analyte has a lower ionization energy than toluene. Proton transfer in reaction R2 will be exothermic when the PA of the analyte is larger than the PA of toluene. For reaction R3, the enthalpy change can be calculated as

$$\Delta H = IE(H) + D(C_6H_5CH_2 - H) - PA(A) - IE(C_7H_8) \quad (S1)$$

where IE stands for ionization energy, D for the dissociation energy of C<sub>sp3</sub>-H bonds, and A represents the analyte molecule.<sup>1</sup> The IE of H is 13.598 eV<sup>2</sup> and the dissociation energy of C<sub>6</sub>H<sub>5</sub>CH<sub>2</sub>-H is 375.5 kJ/mol (3.891 eV).<sup>3</sup> The molecules of interest here were all detected as proton transfer products. Consistent with this observation, toluene's PA is 784.0 kJ/mol (8.123 eV) and its IE is 8.828 eV<sup>2</sup> while methyl ethyl ketone (one of the reference compounds) has a PA of 827.3 kJ/mol<sup>4</sup> (8.574 eV) and an IE of 9.52 eV,<sup>5</sup> implying that methyl ethyl ketone should be detected as a proton transfer product and not a charge transfer product. We see no evidence of fragmentation of the parent VMS compounds.

### 3. Results from Individual Experiments

The results from individual experiments are reported in Tables S1 and S2.

**Table S1** Slopes and two least-squares standard deviations from each experiment performed with OH as the oxidant (asterisks signify experiments where a VMS was used as a reference compound, eliminating that VMS from analysis).

Reference	L2	L3	L4	L5	D3	D4	D5
Propionic Acid	0.89±0.04	1.27±0.07	1.66±0.07	2.28±0.09	0.55±0.02	0.87±0.03	1.41±0.04
Propionic Acid	0.95±0.04	1.29±0.07	1.57±0.07	2.36±0.09	0.56±0.03	0.87±0.03	1.50±0.03
Propionic Acid	0.74±0.04	1.26±0.08	1.67±0.09	2.4±0.1	0.5±0.03	0.96±0.02	1.56±0.03
MEK	1.12±0.05	1.50±0.09	2.2±0.1	2.8±0.1	0.75±0.04	1.17±0.04	2.01±0.04
MEK	1.10±0.04	1.59±0.07	2.24±0.09	3.1±0.1	0.79±0.04	1.16±0.05	1.90±0.05
MEK	1.04±0.07	1.6±0.1	2.3±0.1	3.4±0.2	0.83±0.05	1.29±0.06	2.12±0.08
VMS	*	1.34±0.06	1.93±0.04	2.49±0.05	*	1.57±0.07	2.55±0.09
VMS	*	1.42±0.05	1.86±0.05	2.55±0.05	*	1.57±0.08	2.7±0.1
VMS	*	1.37±0.06	1.66±0.05	2.50±0.04	*	1.46±0.08	2.4±0.1
VMS	*	1.45±0.05	2.03±0.05	2.78±0.05	*	1.67±0.08	2.7±0.1
VMS	*	1.55±0.06	2.3±0.1	3.3±0.2	*	1.54±0.08	2.7±0.1
VMS	*	1.51±0.08	1.99±0.07	2.89±0.08	*	1.56±0.08	2.6±0.1

**Table S2** Slopes and two least-squares standard deviations from each experiment performed with Cl as the oxidant.

Reference	L2	L3	L4	L5	D3	D4	D5
Ether	0.55±0.01	0.72±0.02	0.82±0.02	1.02±0.02	0.18±0.01	0.47±0.02	0.76±0.03
Ether	0.56±0.02	0.71±0.02	0.85±0.02	1.17±0.02	0.24±0.03	0.44±0.02	0.73±0.02
Ether	0.57±0.02	0.70±0.02	0.80±0.02	1.17±0.02	0.21±0.02	0.48±0.01	0.70±0.02
MEK	4.1±0.2	5.0±0.3	6.2±0.4	7.3±0.4	1.5±0.1	3.1±0.2	4.3±0.3
MEK	4.3±0.2	5.1±0.5	5.8±0.6	7.6±0.7	1.4±0.1	3.1±0.2	4.9±0.3
MEK	4.2±0.9	5±1	6±1	8±1	1.4±0.1	3.1±0.2	4.5±0.1

#### 4. Comparison to Literature Values

The rate constants measured in this work for Cl atom-initiated oxidation are compared to the one available literature value in Figure S2.

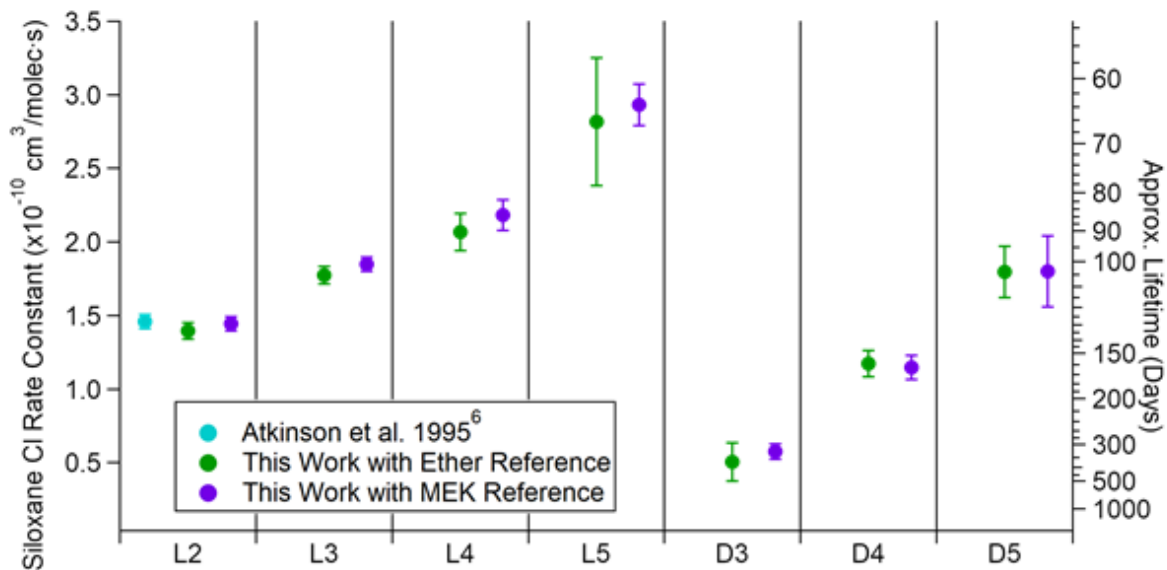


**Figure S2** A comparison of rate constants of VMS with Cl atoms measured in this work with MEK and diethyl ether as reference compounds to one measurement of L2 by Atkinson et al. (1995).<sup>6</sup> Error bars are two standard deviations and do not include the uncertainty of the reference compound's rate constant. The lifetime axis was calculated assuming a 24-hour average Cl concentration of 620 molec cm<sup>-3</sup>.<sup>7</sup>

#### 5. Structure Activity Relationship

As expected for a hydrogen abstraction reaction, the rate constants of individual VMS are related to the number of methyl groups (Figure S3). This analysis shows that OH radical rate constants increase equally between linear and cyclic VMS, but with Cl atoms the rate constants increase faster with cyclic VMS than linear VMS on a per methyl basis.

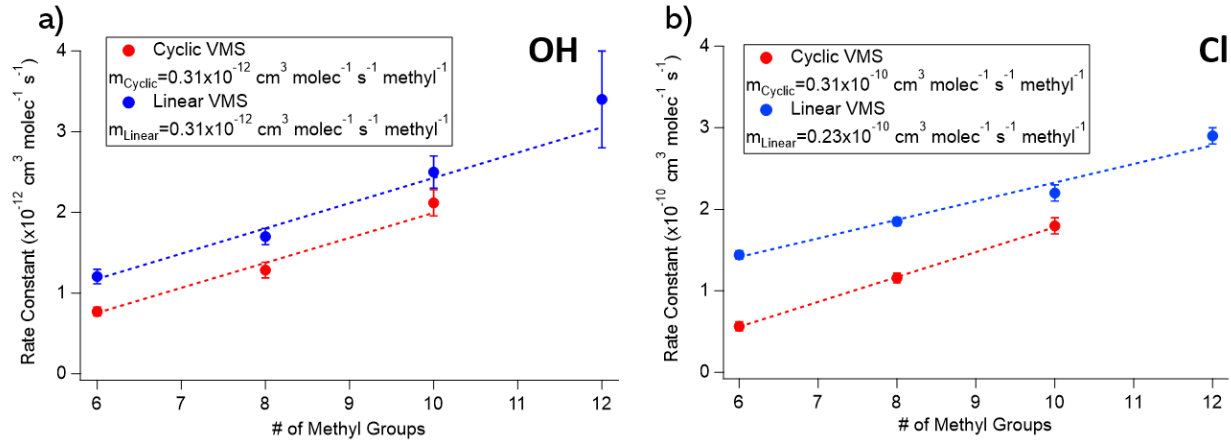


**Figure S3** Plot of the rate constants with (a) OH radicals and (b) Cl atoms presented in this work against the number of methyl groups the VMS has. Dashed lines are weighted least orthogonal distance regressions, with the slopes of the lines reported in the legends.

In addition to expanding  $F(\text{Si})$  to  $F(-\text{Si}(\text{CH}_3)_2\text{OR})$  and  $F(-\text{SiCH}_3(\text{OR})_2)$ , the factors  $F(\text{Si}_{\text{Cyclic}})$  and  $F(\text{Si}_{\text{Linear}})$ , where methyl groups were classified by the structure of the VMS, were also tested. Using factors  $F(\text{Si}_{\text{Cyclic}})$  and  $F(\text{Si}_{\text{Linear}})$  led to a systematic positive offset of rate constants calculated by the SAR, as seen in Figure S4. The fit allowed the intercept to vary; no improvement in results was found when forcing the fit through the origin and suggesting that this model is unable to capture the full reactivity of VMS molecules.  $F(\text{Si}_{\text{Cyclic}})$  is 2.2 while  $F(\text{Si}_{\text{Linear}})$  is 2.5.

The root mean square error (RMSE) was calculated for all SARs by equation S2.

$$RMSE = \sqrt{\frac{\sum_1^n (\text{Modeled} - \text{Measured})^2}{n}} \quad (S2)$$

The RMSE of the AOPWIN SAR is 0.81, using  $F(\text{Si}_{\text{cyclic}})$  and  $F(\text{Si}_{\text{Linear}})$  it is 0.87, while using  $F(-\text{Si}(\text{CH}_3)_2\text{OR})$  and  $F(-\text{SiCH}_3(\text{OR})_2)$  it is 0.34.

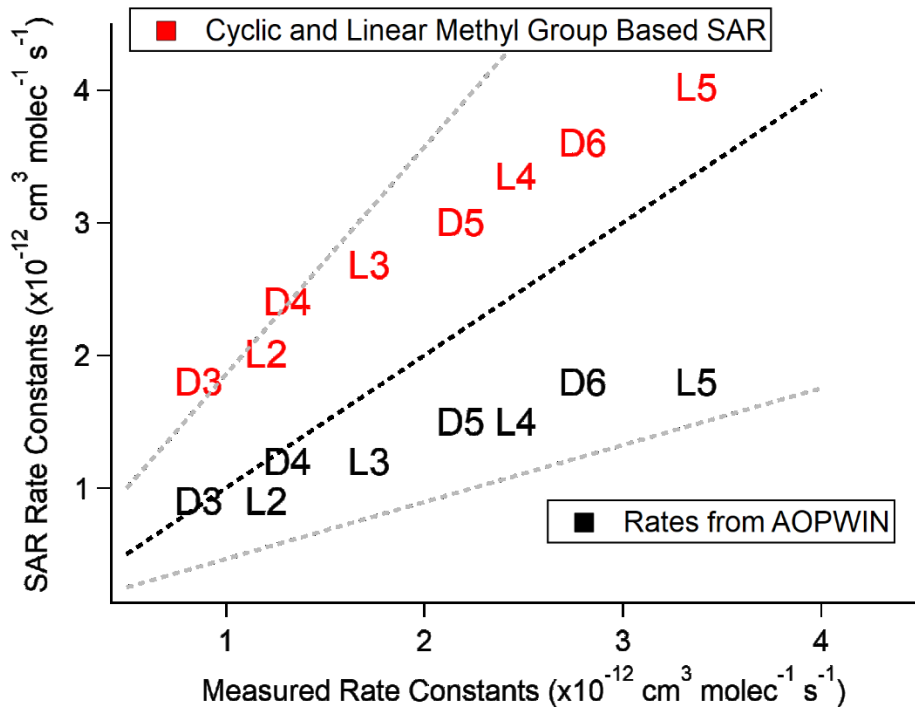
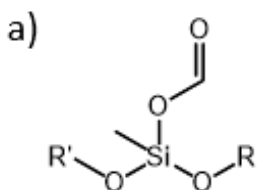


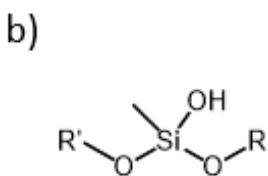
**Figure S4** Plot of AOPWIN rate constants versus measured rate constants in addition to this work's SAR using cyclic and linear VMS methyl groups as the fitted parameter versus measured rate constants. Measured rate constant for D6 is from Safron et al.<sup>8</sup> Dashed black line represents a 1:1 relationship and the two dashed grey lines are 2:1 and 0.5:1.

## 6. Siloxane Product Structures and General Formulas

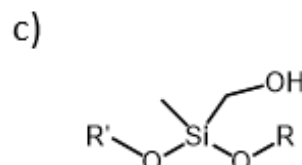
For clarity, general structures with the formulas of the VMS oxidation products are shown in Figure S5.



Name: Formate ester  
Formula:  $\text{Si}(\text{OR})_2(\text{CH}_3)(\text{OC(O)H})$



Name: Silanol  
Formula:  $\text{Si}(\text{OR})_2(\text{CH}_3)(\text{OH})$



Name: Silyl methanol  
Formula:  $\text{Si}(\text{OR})_2(\text{CH}_3)(\text{CH}_2\text{OH})$

**Figure S5** General structures, names, and formulas for (a) the formate ester product, (b) the silanol product, and (c) the silyl methanol product that was proposed but not identified in this work.

## 7. Urban Cl Atom Impacts

As a recent study has shown that D5 potentially has a diurnal profile in urban environments,<sup>9</sup> the impact of the coincidental increase in Cl atom and D5 concentration on the importance of Cl atom oxidation was investigated. Using approximations of these diurnal profiles, the cumulative percent loss of D5 was calculated as a function of hour of day. This calculation determined the amount of D5 that reacted with OH radicals or Cl atoms at each time point, using concentrations of OH radicals and Cl atoms similar to the concentrations measured during the CalNex campaign.<sup>10</sup> The cumulative amount of oxidized D5 formed via reactions with OH radicals and Cl atoms were tracked separately over the course of the day. Figure S6 shows the amount of oxidized VMS from Cl atoms, the amount of oxidized D5 from OH radicals, and the total amount of D5 oxidized.

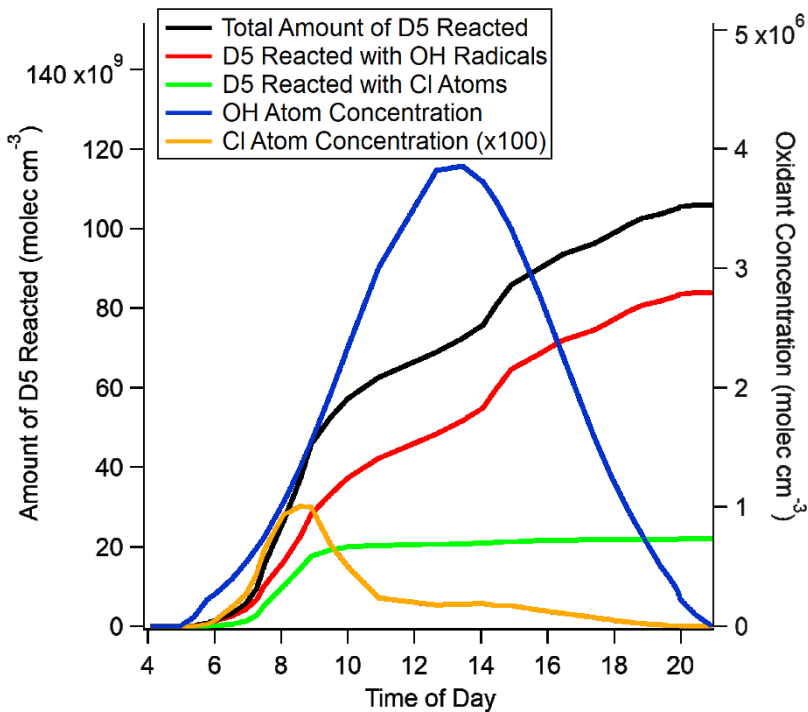


**Figure S6** Using the diurnal profile of D5 from Toronto, CA from Coggon et al. (2018),<sup>9</sup> and the measured Cl atom concentration with the  $[\text{OH}]/[\text{Cl}]$  ratio from Young et al. (2014),<sup>10</sup> the amount of D5 that reacts with Cl atoms and OH radicals was calculated and summed over the course of a day.

To calculate a cumulative percent loss of D5 to Cl atoms over a day, the Cl atom channel of oxidized VMS formation (green trace) was divided by the cumulative D5 lost (black trace) via oxidation over the course of the day. Diurnal profiles of D5 have been measured in two cities, with a much clearer diurnal variation in Toronto, Canada than in Boulder, CO, USA. A graph of the results is shown in figure S7. Cl atoms are most important in the early mornings, with Cl atoms contributing to more than 30% of the D5 oxidation by 9am, but about 25% by noon.

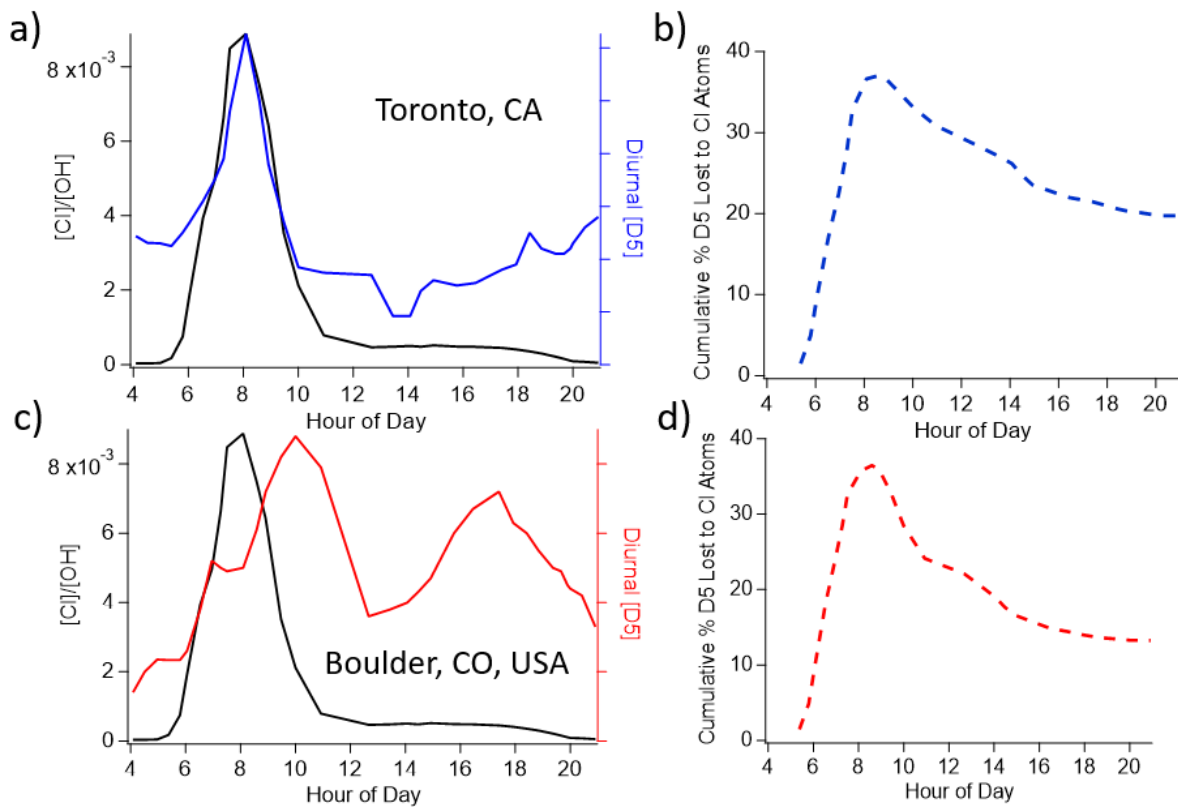


**Figure S7** (a) Diurnal profiles of D5 in Toronto, Canada, from Coggon et al. (2018) and Cl atom to OH radical ratio from Young et al. (2014) used in this calculation. (b) Cumulative percent contribution of Cl atoms to D5 oxidation over the time period for which the diurnal profiles in Toronto, Canada are available. (c) The same figure as in (a), but with diurnal profile measured in Boulder, CO, USA. (d) Cumulative percent contribution of Cl atoms to D5 oxidation in Boulder, CO.

## References

- (1) Herrera, L. C.; Grossert, J. S.; Ramaley, L. Quantitative Aspects of and Ionization Mechanisms in Positive-Ion Atmospheric Pressure Chemical Ionization Mass Spectrometry. *J. Am. Soc. Mass Spectrom.* **2008**, *19* (12), 1926–1941. <https://doi.org/10.1016/j.jasms.2008.07.016>.
- (2) Lias, S. G. *Ionization Energy Evaluation*; Linstrom, P. J., Mallard, W. G., Eds.; National Institute of Standards and Technology: Gaithersburg, MD. <https://doi.org/https://doi.org/10.18434/T4D303>.
- (3) Rumble, J. R. ed. *Handbook of Chemistry and Physics, 100th Edition*, Internet V.; CRC press/Taylor & Francis: Boca Raton, FL, 2019.
- (4) Hunter, E. P.; Lias, S. G. Evaluated Gas-Phase Basicities and Proton Affinities of Molecules: An Update. *J. Phys. Chem. Ref. Data* **1998**, *27* (3), 413–656. <https://doi.org/10.1063/1.556018>.
- (5) Traeger, J. C. Heat of Formation for the Propanoyl Cation by Photoionization Mass Spectrometry. *Org. Mass Spectrom.* **1985**, *20* (3), 223–227. <https://doi.org/10.1002/oms.1210200311>.
- (6) Atkinson, R.; Tuazon, E. C.; Kwok, E. S. C.; Arey, J.; Aschmann, S. M.; Bridier, I. Kinetics and Products of the Gas-Phase Reactions of  $(CH_3)_4Si$ ,  $(CH_3)_3SiCH_2OH$ ,  $(CH_3)_3SiOSi(CH_3)_3$  and  $(CD_3)_3SiOSi(CD_3)_3$  with Cl Atoms and OH Radicals. *J. Chem. Soc. Faraday Trans.* **1995**, *91* (18), 3033. <https://doi.org/10.1039/ft9959103033>.
- (7) Wang, X.; Jacob, D. J.; Eastham, S. D.; Sulprizio, M. P.; Zhu, L.; Chen, Q.; Alexander, B.; S11

Sherwen, T.; Evans, M. J.; Lee, B. H.; Haskins, J. D.; Lopez-Hilfiker, F. D.; Thornton, J. A.; Huey, G. L.; Liao, H. The Role of Chlorine in Global Tropospheric Chemistry. *Atmos. Chem. Phys.* **2019**, *19* (6), 3981–4003. <https://doi.org/10.5194/acp-19-3981-2019>.

(8) Safron, A.; Strandell, M.; Kierkegaard, A.; Macleod, M. Rate Constants and Activation Energies for Gas-Phase Reactions of Three Cyclic Volatile Methyl Siloxanes with the Hydroxyl Radical. *Int. J. Chem. Kinet.* **2015**, *47* (7), 420–428. <https://doi.org/10.1002/kin.20919>.

(9) Coggon, M. M.; McDonald, B. C.; Vlasenko, A.; Veres, P. R.; Bernard, F.; Koss, A. R.; Yuan, B.; Gilman, J. B.; Peischl, J.; Aikin, K. C.; DuRant, J.; Warneke, C.; Li, S.; de Gouw, J. A. Diurnal Variability and Emission Pattern of Decamethylcyclopentasiloxane (D5) from the Application of Personal Care Products in Two North American Cities. *Environ. Sci. Technol.* **2018**, *52* (10), 5610–5618. <https://doi.org/10.1021/acs.est.8b00506>.

(10) Young, C. J.; Washenfelder, R. A.; Edwards, P. M.; Parrish, D. D.; Gilman, J. B.; Kuster, W. C.; Mielke, L. H.; Osthoff, H. D.; Tsai, C.; Pikelnaya, O.; Stutz, J.; Veres, P. R.; Roberts, J. M.; Griffith, S.; Dusanter, S.; Stevens, P. S.; Flynn, J.; Grossberg, N.; Lefer, B.; Holloway, J. S.; Peischl, J.; Ryerson, T. B.; Atlas, E. L.; Blake, D. R.; Brown, S. S. Chlorine as a Primary Radical: Evaluation of Methods to Understand Its Role in Initiation of Oxidative Cycles. *Atmos. Chem. Phys.* **2014**, *14* (7), 3427–3440. <https://doi.org/10.5194/acp-14-3427-2014>.